Strange dibaryon resonance in the $\bar{K}NN$-πYN system

Y. Ikeda and T. Sato*

Department of Physics, Graduate School of Science, Osaka University, Toyonaka, Osaka 560-0043, Japan

(Received 18 April 2007; revised manuscript received 12 July 2007; published 5 September 2007)

Three-body resonances in the $\bar{K}NN$ system have been studied within a framework of the $\bar{K}NN$-πYN coupled-channel Faddeev equation. By solving the three-body equation, the energy dependence of the resonant $\bar{K}N$ amplitude is fully taken into account. The S-matrix pole has been investigated from the eigenvalue of the kernel with the analytic continuation of the scattering amplitude on the unphysical Riemann sheet. The $\bar{K}N$ interaction is constructed from the leading order term of the chiral Lagrangian using relativistic kinematics. The $\Lambda(1405)$ resonance is dynamically generated in this model, where the $\bar{K}N$ interaction parameters are fitted to the data of scattering length. As a result we find a three-body resonance of the strange dibaryon system with binding energy $B \sim 79$ MeV and width $\Gamma \sim 74$ MeV. The energy of the three-body resonance is found to be sensitive to the model of the $I = 0$ $\bar{K}N$ interaction.

DOI: 10.1103/PhysRevC.76.035203 PACS number(s): 13.75.Jz, 11.30.Rd, 11.80.Jy, 14.20.Pt

I. INTRODUCTION

The analysis of the kaonic atoms [1] has revealed an attractive $\bar{K}$-nucleus interaction. Although the strength of the attraction depends on the parametrization of the density dependence of the optical potential [1] and the theoretical study of the $\bar{K}$ optical potential suggests a rather shallow potential [2], there has been a great interest in the possibilities of $\bar{K}$-nucleus bound states in recent years. Akaishi and Yamazaki [3,4] studied the kaon bound states in light nuclei and found deeply bound kaonic states, for example, $B \sim 100$ MeV for ${}^{3}_{\bar{K}}\mathrm{H}$. In their study, the kaonic nuclear states were investigated by using the $\bar{K}$ optical potential, which is constructed by folding the g matrix with a trial nuclear density. The potential model of the $\bar{K}N$-$\pi\Sigma$ interaction is determined to reproduce the $\Lambda(1405)$ and the scattering length. The kaonic nuclear states are further studied by using a method of antisymmetrized molecular dynamics [5] using the $\bar{K}N$ g matrix.

Among the simplest $\bar{K}$ nucleus state, the $K^- pp$ state, which has strangeness $S = -1$, total angular momentum and parity $J^\pi = 0^-$, and isospin $I = 1/2$ dibaryon state, is expected to have the largest component of the $I = 0$ $\bar{K}N$. An experimental signal of the $K^- pp$ bound state is reported by the FINUDA Collaboration from the analysis of the invariant mass distribution of Λ-p in the K^- absorption reaction on nuclei [6]. The reported central value of the binding energy B and the width Γ are $(B, \Gamma) = (115, 67)$ MeV, which is below the $\pi\Sigma N$ threshold energy. These data may be compared with the predicted values $(B, \Gamma) = (48, 61)$ MeV in Ref. [4]. However, it has been pointed out that the data can be understood by the two-nucleon absorption of K^- in nuclei together with the final state interaction of the outgoing baryons [7].

In the attractive interaction of kaon in nuclei, the resonance $\Lambda(1405)$ in the s-wave and $I = 0$ channel $\bar{K}N$ scattering state plays an essential role. The energy of the $\Lambda(1405)$ is below the $\bar{K}N$ threshold and strongly couples with the $\pi\Sigma$ state. Although the kaonic nuclear states have been studied so far by using the $\bar{K}N$ g matrix or optical potential, it might be very important to examine the full dynamical calculation of $\bar{K}N$-$\pi\Sigma$ system by taking into account the energy dependence of the resonance t matrix and the coupling with the $\bar{K}N$-$\pi\Sigma$ channel explicitly. Such a theoretical study may be possible in the simplest kaonic nuclei with baryon number $B = 2$ system. In this work, we study the strange dibaryon system by taking into account the three-body dynamics using the $\bar{K}NN$-$\pi\Sigma N$-$\pi\Lambda N$ ($\bar{K}NN$-πYN) coupled-channel Faddeev equation with relativistic and nonrelativistic kinematics.

Methods to investigate resonances in the three-body system have been developed in the studies of the three-neutron [8,9], πNN dibaryon [10,11] and ΣNN hypernuclei [10,12,13]. In this work, we employ a method started by Glöckle [8] and Möller [9] and developed by Matsuyama and Yazaki [10] and Afnan, Pearce, and Gibson [12,13] to find a pole of the S matrix in the unphysical energy plane from the eigenvalue of the kernel of the Faddeev equation. To analytically continue the scattering amplitude into the unphysical sheet, the path of the momentum integral must be carefully deformed in the complex plane to avoid possible singularities.

The most important interaction for the study of the strange dibaryon system is for the $I = 0$ $\bar{K}N$ states. The internal structure of the $\Lambda(1405)$ has been a long standing issue. The chiral Lagrangian approach [14–16] can describe well the low energy $\bar{K}N$ reaction with the meson-baryon dynamics. A genuine q^3 picture of the $\Lambda(1405)$ coupled with meson-baryon [17] may not yet be excluded. Though previous studies of the $\bar{K}NN$ system used phenomenological models of the $\bar{K}N$ potentials, we use s-wave meson-baryon coupled-channel potentials guided by the lowest order chiral Lagrangian. With this model, the strength of the potentials and the relative strength of the potentials among various meson-baryon channels are not parameters but are determined from the SU(3) structure of the chiral Lagrangian. In this model, the $\Lambda(1405)$ is an "unstable bound state," whose pole on the unphysical sheet will become the bound state of $\bar{K}N$ when the coupling between the $\bar{K}N$ and the πY is turned off. We examine a relativistic model as well as a nonrelativistic model to account for the relativistic energy of pion in the πYN state.

*ikeda@kern.phys.sci.osaka-u.ac.jp, tsato@phys.sci.osaka-u.ac.jp

We briefly explain our $\bar{K}NN$-πYN coupled-channel equations and the procedure to search for the three-body resonance in Sec. II. The model of the two-body interactions used in this work is explained in Sec. III. We then report our results on the $\bar{K}NN$ dibaryon resonance in Sec. IV. This work is the extension of the early version of our analysis reported in Ref. [18]. Recently Shevchenko *et al.* [19] performed a similar study of the $\bar{K}NN$ system using the Faddeev equation starting from the phenomenological $\bar{K}N$ interaction within a nonrelativistic framework. The comparison of our results with theirs will be discussed in Sec. IV.

II. COUPLED-CHANNEL FADDEEV EQUATION AND RESONANCE POLE

We start from the Alt-Grassberger-Sandhas (AGS) equation [20] for the three-body scattering problem. The operators $U_{i,j}$ of the three-body scattering satisfy the AGS equation

$$U_{i,j} = (1-\delta_{i,j})G_0^{-1} + \sum_{n\neq i} t_n G_0 U_{n,j}. \tag{1}$$

Here we label the pair of particles j,k by the spectator particle $i=1,2,3$. The two-body t matrix t_i of particles j,k with the spectator particle i is given by the solution of the Lippmann-Schwinger equation

$$t_i = v_i + v_i G_0 t_i. \tag{2}$$

Here $G_0 = 1/(W - H_0 + i\epsilon)$ is the free Green's function of the three particles, and W is the total energy of the three-body system.

When the two-body interactions v_i are given in separable form with the vertex form factor $|g_i\rangle$ and the coupling constant γ_i as

$$v_i = |g_i\rangle \gamma_i \langle g_i|, \tag{3}$$

the AGS equation (1) is written in the form

$$\begin{aligned} X_{i,j}(\vec{p}_i,\vec{p}_j,W) &= (1-\delta_{i,j})Z_{i,j}(\vec{p}_i,\vec{p}_j,W) \\ &\quad + \sum_{n\neq i}\int d\vec{p}_n Z_{i,n}(\vec{p}_i,\vec{p}_n,W) \\ &\quad \times \tau_n(W) X_{n,j}(\vec{p}_n,\vec{p}_j,W). \end{aligned} \tag{4}$$

The amplitude $X_{i,j}$ is defined by the matrix element of $U_{i,j}$ between state vectors $G_0|\vec{p}_i, g_i\rangle$ as

$$X_{i,j}(\vec{p}_i,\vec{p}_j,W) = \langle \vec{p}_i, g_i | G_0 U_{i,j} G_0 | \vec{p}_j, g_j\rangle. \tag{5}$$

The state vector $|\vec{p}_i, g_i\rangle$ represents a plane wave state of the spectator i and the state vector $|g_i\rangle$ of the interacting pair.

The driving term $Z_{i,j}$ of Eq. (4) shown in Fig. 1(a) is given by the particle exchange mechanism defined as

$$Z_{i,j}(\vec{p}_i,\vec{p}_j,W) = \langle \vec{p}_i, g_i | G_0 | \vec{p}_j, g_j\rangle \tag{6}$$

$$= \frac{g^*(\vec{q}_i) g(\vec{q}_j)}{W - E_i(\vec{p}_i) - E_j(\vec{p}_j) - E_k(\vec{p}_k)}. \tag{7}$$

Here the momentum of the exchanged particle $k(\neq i,j)$ is given as $\vec{p}_k = -\vec{p}_i - \vec{p}_j$, and $g(\vec{q}_i)$ is the vertex form factor of the two-body interaction $g(\vec{q}_i) = \langle g_i | \vec{q}_i\rangle$. The energy $E_i(\vec{p}_i)$ is given by $E_i(\vec{p}_i) = m_i + \vec{p}_i^{\,2}/2m_i$ for the nonrelativistic model and $E_i(\vec{p}_i) = \sqrt{m_i^2 + \vec{p}_i^{\,2}}$ for the relativistic model. The relative momentum is given by $\vec{q}_i = (m_k\vec{p}_j - m_j\vec{p}_k)/(m_j+m_k)$ for the nonrelativistic model, while we define $q_i = |\vec{q}_i|$ for the relativistic model as

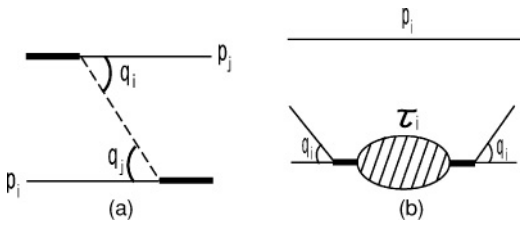

FIG. 1. Graphical representation of (a) one particle exchange interaction $Z_{i,j}(\vec{p}_i,\vec{p}_j,W)$ and (b) two-body t matrix $\tau_i(W)$. The relative momentum of the interacting particles is given by $\vec{q}_i$ for spectator particle i.

$$q_i = \sqrt{\left(\frac{W_i^2 + m_j^2 - m_k^2}{2W_i}\right)^2 - m_j^2}, \tag{8}$$

$$W_i = \sqrt{(E_j(\vec{p}_j) + E_k(\vec{p}_k))^2 - \vec{p}_i^{\,2}}. \tag{9}$$

The two-body t matrix can be solved for the separable interaction as

$$t_i = |g_i\rangle \tau_i(W) \langle g_i|. \tag{10}$$

Here the "isobar" propagator τ_i, illustrated in Fig. 1(b), is given as

$$\tau_i(W) = \left[1/\gamma_i - \int d\vec{q}_i \frac{|g_i(\vec{q}_i)|^2}{W - E_i(\vec{p}_i) - E_{jk}(\vec{p}_i,\vec{q}_i)}\right]^{-1}. \tag{11}$$

The two-body t matrix depends on the energy $E_i(\vec{p}_i)$ of the spectator particle. Here E_{jk} is the energy of the interacting pair given as $E_{jk}(\vec{p}_i,\vec{q}_i) = m_j + m_k + \vec{p}_i^{\,2}/(m_j+m_k) + \vec{q}_i^{\,2}/\mu_i$ for the nonrelativistic model, while $E_{jk}(\vec{p}_i,\vec{q}_i) = \sqrt{(E_j(\vec{q}_i) + E_k(\vec{q}_i))^2 + \vec{p}_i^{\,2}}$ for the relativistic model. The reduced mass is defined as $\mu_i = m_j m_k/(m_j+m_k)$.

Following the standard method of angular momentum expansion [21], the AGS equation reduces to the following coupled integral equation by keeping only s-wave states:

$$\begin{aligned} X_{i,j}(p_i,p_j,W) &= Z_{i,j}(p_i,p_j,W) + \sum_n \int dp_n p_n^2 \\ &\quad \times K_{i,n}(p_i,p_n,W) X_{n,j}(p_n,p_j,W). \end{aligned} \tag{12}$$

Here we used a simplified notation for the kernel $K = Z\tau$, which can be written as

$$K_{i,n}(p_i, p_n, W) = 2\pi \int d(\hat{p}_i \cdot \hat{p}_n) \frac{g^*(q_i)g(q_n)}{W - E_i(p_i) - E_j(p_n) - E_k(\vec{p}_i + \vec{p}_n)} \tau_n(W). \tag{13}$$

The formulas given above are valid for the spinless and distinguishable particles without channel coupling among the Fock-space vectors. In our $\bar{K}NN$ resonance problem, we have included the following $\bar{K}NN$ and πYN states:

$$|a\rangle = |N_1, N_2, \bar{K}_3\rangle, \tag{14}$$

$$|b\rangle = |N_1, Y_2, \pi_3\rangle, \tag{15}$$

$$|c\rangle = |Y_1, N_2, \pi_3\rangle, \tag{16}$$

with Y_i is Σ_i or Λ_i. After antisymmetrizing the amplitude for identical particles of nucleons [11], we obtain the following forms of the coupled AGS equations:

$$\begin{pmatrix} X_{Y_K,Y_K} \\ X_{Y_\pi,Y_K} \\ X_{d,Y_K} \\ X_{N^*,Y_K} \end{pmatrix} = \begin{pmatrix} Z_{Y_K,Y_K} \\ 0 \\ Z_{d,Y_K} \\ 0 \end{pmatrix} + \begin{pmatrix} -Z_{Y_K,Y_K}\tau_{Y_K,Y_K} & -Z_{Y_K,Y_K}\tau_{Y_K,Y_\pi} & 2Z_{Y_K,d}\tau_{d,d} & 0 \\ 0 & 0 & 0 & -Z_{Y_\pi,N^*}\tau_{N^*,N^*} \\ Z_{d,Y_K}\tau_{Y_K,Y_K} & Z_{d,Y_K}\tau_{Y_K,Y_\pi} & 0 & 0 \\ -Z_{N^*,Y_\pi}\tau_{Y_\pi,Y_K} & -Z_{N^*,Y_\pi}\tau_{Y_\pi,Y_\pi} & 0 & 0 \end{pmatrix} \begin{pmatrix} X_{Y_K,Y_K} \\ X_{Y_\pi,Y_K} \\ X_{d,Y_K} \\ X_{N^*,Y_K} \end{pmatrix}. \tag{17}$$

Here, we have suppressed the spin-isospin quantum numbers, the spectator momentum p_j, and the total energy of the three-body system W in Z, X, and τ for simplicity. The concise notation of Y_K, Y_π, d, and N^* represents the "isobars" and their decay channels. The decay channels of isobars Y_K, Y_π, d, and N^* are $\bar{K}N(I = 0, 1), \pi\Sigma(I = 0, 1)$ and $\pi\Lambda(I = 1), NN(I = 1)$ and $\pi N(I = 1/2, 3/2)$, respectively. Here, I is the isobar isospin. Those indices uniquely specify the three-body states of X and Z except for N^* showing ΣN^* and ΛN^*. Therefore we have a nine-channel coupled equation of Eq. (17) for the spin singlet, s-wave three-body system. The explicit form of Eq. (7) when we include spin-isospin is summarized in the Appendix.

The dominant Fock space component is expected to be $|\bar{K}NN\rangle$, and therefore the most important amplitudes are X_{Y_K,Y_K} and X_{d,Y_K}. They couple to each other through the kaon exchange Z_{Y_K,Y_K} and nucleon exchange $Z_{Y_K,d}$ mechanisms. Notice, however, that the πYN component is also implicitly included in τ_{Y_K,Y_K} when we solve the two-body $\bar{K}N$-πY coupled-channel equations. The πYN components, $X_{Y\pi,Y_K}$ and X_{N^*,Y_K}, couple with the $\bar{K}NN$ components through the pion exchange mechanism Z_{N^*,Y_π} and the πN and πY isobars $\tau_{N^*,N^*}, \tau_{Y_\pi,Y}$. The pion exchange mechanism may play an important role in the width of the resonance. In this work, we have not included the weak YN interaction. It was found in Ref. [19] that the YN interaction plays a rather minor role in this strange dibaryon system.

To find the resonance energy of the three-body system using the AGS equation of Eq. (17), we follow the method used in Refs. [8–10,12,13]. The AGS equation of Eq. (13) is a Fredholm-type integral equation with the kernel $K = Z\tau$. Using the eigenvalue $\eta_a(W)$ and the eigenfunction $|\phi_a(W)\rangle$ of the kernel for given energy W,

$$Z\tau|\phi_a(W)\rangle = \eta_a(W)|\phi_a(W)\rangle, \tag{18}$$

the scattering amplitude X can be written as

$$X = \sum_a \frac{|\phi_a(W)\rangle\langle\phi_a(W)|Z}{1 - \eta_a(W)}. \tag{19}$$

At the energy $W = W_p$ where $\eta_a(W_p) = 1$, the amplitude has a pole, and therefore W_p gives the bound state or resonance energy.

Since a resonance pole appears on the unphysical energy Riemann sheet, we need analytic continuation of the scattering amplitude. We use here the nonrelativistic model to explain a method of analytic continuation, which is based on Refs. [9,10]. At first we examine the singularities of the kernel of Eq. (13). Above the threshold energy of the three-body breakup $W > m_i + m_j + m_k$, $Z(p_i, p_n, W)$ has logarithmic singularities. The branch points appear at $p_n = \pm p_{Z_{1,2}}$, where

$$p_{Z_1} = -\frac{\mu_j}{m_k} p_i + \sqrt{2\mu_j W_{\rm th} - \frac{\mu_j}{\eta_j} p_i^2}, \tag{20}$$

$$p_{Z_2} = +\frac{\mu_j}{m_k} p_i + \sqrt{2\mu_j W_{\rm th} - \frac{\mu_j}{\eta_j} p_i^2}, \tag{21}$$

with

$$\mu_j = \frac{m_i m_k}{m_i + m_k},$$
$$\eta_j = \frac{m_j(m_i + m_k)}{m_i + m_j + m_k},$$
$$W_{\rm th} = W - m_i - m_j - m_k.$$

For given $p_i > 0$, the cuts run from p_{Z_1} to p_{Z_2} above the positive real axis of the complex p_n plane and from $-p_{Z_1}$ to $-p_{Z_2}$ below the negative real axis as shown in Fig. 2, while the integration of momentum p_n in Eq. (13) is along the real positive axis.

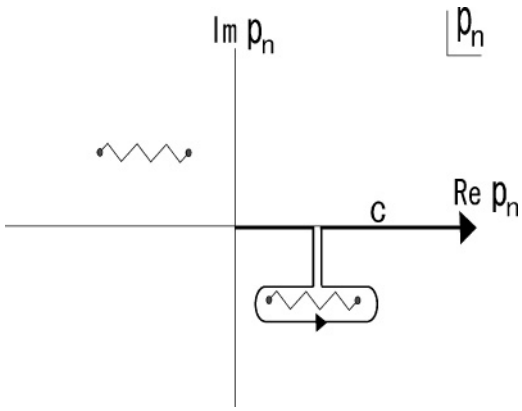

FIG. 2. Singularities of the one particle exchange interaction $Z(p_i, p_n, W)$ in the complex p_n plane at $W = E + i\epsilon$ and the real p_i.

Let us consider the case when W has a negative imaginary part. For given $p_i > 0$, the cut from p_{Z_1} to p_{Z_2} moves into the fourth quadrant across the integration contour of p_n. Assuming the integrand of Eq. (12) is an analytic function around real positive p_n, one can perform an analytic continuation of the amplitudes by deforming the integration contour along the logarithmic singularity as shown in Fig. 3, and then we obtain amplitudes on the unphysical Riemann sheet.

In principle it might be possible to solve the AGS equation keeping the momentum variables real and taking into account the discontinuity across the cut. The moving logarithmic singularities depending on p_i make it difficult to solve the integral equation. To overcome this problem, we deform the integration contour of p_i, p_n, into the fourth quadrant of the complex momentum plane so that we take into account the contribution of the cuts. As an example of our $\bar{K}NN$-πYN problem, we choose the integration contour of p_n as shown in the solid line in Fig. 4. Here we take the energy $W = 10 - i35 + m_\pi + m_\Sigma + m_N$ MeV, which is below the mass of $\bar{K}NN$ and above the πYN. The shaded region in Fig. 4 shows the cuts of Z for the pion exchange mechanism. The cuts become "forbidden regions" because the position of the cuts depends on p_i, which runs the same integration contour as p_n. In our

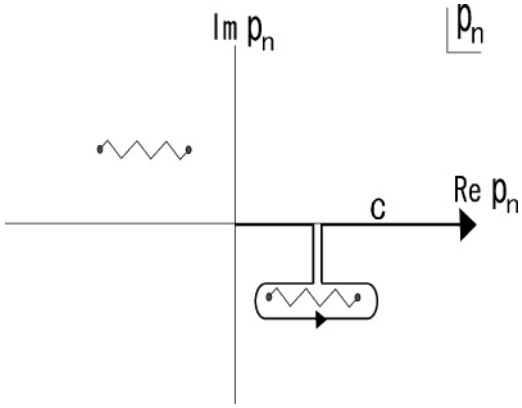

FIG. 3. Integration contour C and the singularity of Z at $W = E - i\Gamma/2$ and real value of p_i.

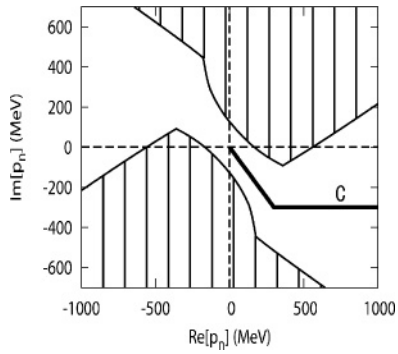

FIG. 4. Logarithmic singularities of the π exchange mechanism $Z(p_i, p_n, Z)$ at $W_{\rm th} = 10 - i35$ MeV in the complex p_n plane. C is the integration contour of p_n and p_i.

numerical calculation, we studied all the forbidden regions for π, N, and K exchange mechanism and determined the integration contour. With the integration contour C in Fig. 4, we choose the physical sheet of $\bar{K}NN$.

The singularities of the isobar propagator $\tau(W)$ arises from the three-body Green's function in the integrand of τ. The poles are at $q_n = \pm\sqrt{2\mu_j W_{\rm th} - \frac{\mu_j}{\eta_j} p_i^2}$. Since $q_s = (p_{Z_1} + p_{Z_2})/2$, we can analytically continue it into the same unphysical sheet as the case in Z as long as we keep the same deformed contour as the one used in Z. Another singularity we have to worry about is that due to the two-body resonance. Since our $\bar{K}N$-$\pi\Sigma$ system has the two-body resonance $\Lambda(1405)$, the cut starts from the two-body resonance energy in the complex energy plane. To examine this, we write the approximate energy dependence of the τ as

$$\tau_i(W) \sim \frac{1}{W - \frac{p_N^2}{2\eta_N} - E_{\Lambda^*} - m_N}. \tag{22}$$

Here p_N and m_N are the momentum and mass of the spectator nucleon. The reduced mass of the spectator nucleon with the isobar pair $\bar{K}N$ or $\pi\Sigma$ is denoted as η_N, and E_{Λ^*} is the pole energy of $\Lambda(1405)$. At $W = \frac{p_N^2}{2\eta_N} + E_{\Lambda^*} + m_N$ with p_N on the contour C in Fig. 5(b), the two-body t matrix has a singularity, which is plotted as a solid line in Fig. 5(a). We illustrate the typical trajectories of the three-body resonance pole $W = W_p$ as curves A and B in Fig. 5. If the pole trajectories A and

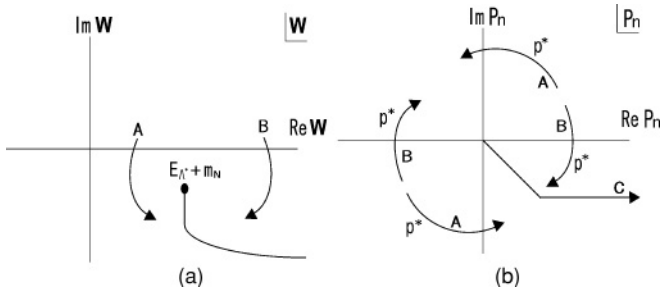

FIG. 5. Singularities due to the three-body resonance and the $\Lambda(1405)$ in (a) the complex energy plane and (b) the momentum plane.

B intercept the two-body $N\Lambda(1405)$ cut, then the analytic continuation to the $N\Lambda(1405)$ unphysical energy sheet must be examined. The same situation from the p_N plane is shown in Fig. 5(b). The momentum p^* corresponding to the energy W_p of the three-body resonance is determined by

$$p^* = \pm\sqrt{2\eta_N(W_p - E_{\Lambda^*} - m_N)}. \tag{23}$$

If p^* intercepts contour C, we have to take care of the analytic continuation of the $N\Lambda(1405)$ energy sheet. As will be seen in Sec. IV, the trajectories of the three-body resonance in our calculation follow line A of Fig. 5(a) and do not intercept the singularity of the two-body resonance.

III. MODEL OF THE TWO-BODY INTERACTIONS

We take into account the $\bar{K}N$ interactions in $J^\pi = 1/2^-$, $I = 0$ and $I = 1$ states; the πN interactions in $J^\pi = 1/2^-$, $I = 1/2$ and $3/2$ states; and the NN interaction in $I = 0$, $^1S_0$ state. Our s-wave meson-baryon interaction is guided by the leading order effective chiral Lagrangian for the octet baryon ψ_B and the pseudoscalar meson ϕ fields given as

$$L_{\rm int} = \frac{i}{8F_\pi^2}{\rm tr}(\bar{\psi}_B\gamma^\mu[[\phi, \partial_\mu\phi], \psi_B]). \tag{24}$$

The meson-baryon potential derived from the chiral Lagrangian can be written as

$$\langle\vec{p}', \beta|V_{BM}|\vec{p}, \alpha\rangle = -C_{\beta,\alpha}\frac{1}{(2\pi)^3 8F_\pi^2} \times \frac{m_\beta + m_\alpha}{\sqrt{4E_\beta(\vec{p}')E_\alpha(\vec{p})}}g_\beta(\vec{p}')g_\alpha(\vec{p}). \tag{25}$$

Here $\vec{p}$ and $\vec{p}'$ are the momentum of the meson in the initial state α and the final state β. The strength of the potential at zero momentum is not an arbitrary constant but is determined by the pion decay constant F_π. The relative strength between the meson-baryon states is controlled by the constants $C_{\beta,\alpha}$ which are basically determined by the SU(3) flavor structure of the chiral Lagrangian. The parameter of our model is the cutoff Λ of the phenomenologically introduced vertex function $g_\alpha(\vec{p}) = \Lambda_\alpha^4/(\vec{p}^2 + \Lambda_\alpha^2)^2$.

The most important interaction for the study of the $\bar{K}NN$ system is the $I = 0$ $\bar{K}N$ interaction. We describe the $\bar{K}N$ interaction by the coupled-channel model of the $\bar{K}N$ and $\pi\Sigma$ states. The constants $C_{\beta,\alpha}$ for this channel are given as $C_{\bar{K}N\text{-}\bar{K}N} = 6$, $C_{\bar{K}N\text{-}\pi\Sigma} = -\sqrt{6}$, and $C_{\pi\Sigma\text{-}\pi\Sigma} = 8$. The cutoff Λ is determined by fitting the scattering length $a_{\bar{K}N}^{I=0} = -1.70 + i0.68$ fm of Ref. [22]. The values of Λ are around 1 GeV and are given as model (a) in Tables I and II for the nonrelativistic and the relativistic models. In general, the form factors of the relativistic models are hard compared with those of the nonrelativistic models because of the weak relativistic kinetic energy. We found a resonance pole at $W = 1420 - i30$ MeV for the nonrelativistic and relativistic models. The relativistic kinematics might be important in describing the πY channel because of the small pion mass. We choose this model (a) as a standard parameter of the $\bar{K}N$ interaction.

TABLE I. Cutoff parameters, scattering lengths, and resonance poles of the relativistic models of the $I = 0$, $\bar{K}N$-$\pi\Sigma$ interaction.

Model	$\bar{K}N$ (MeV)	$\pi\Sigma$ (MeV)	Scattering length (fm)	Resonance energy (MeV)
(a)	1095	1450	$-1.70 + i0.68$	$1419.8 - i29.4$
(b)	1105	1550	$-1.60 + i0.68$	$1422.2 - i33.7$
(c)	1085	1350	$-1.80 + i0.68$	$1418.5 - i25.0$
(d)	1120	1340	$-1.70 + i0.59$	$1414.6 - i29.4$
(e)	1070	1540	$-1.70 + i0.78$	$1424.3 - i28.3$
(f)	1160	1100	$-1.72 + i0.44$	$1405.8 - i25.2$

The $\bar{K}N$ scattering lengths are not very well constrained from the data. The ranges of the $\bar{K}N$ scattering lengths are studied within the chiral unitary model in Ref. [23]. In this work, we simply examined models with the scattering length $a_{\bar{K}N}^{I=0} = (-1.70 \pm 0.10) + i(0.68 \pm 0.10)$ fm in order to examine the sensitivity of the energy of the three-body resonance on the input model of the two-body interaction. The cutoff Λ's for those models are given as models (b)–(e) of Tables I and II. The values of the resonance energy are about $1415 \sim 1425$ MeV, and the width $50 \sim 70$ MeV, which are close to the values of the chiral model in Ref. [16]. One can notice that there is a correlation between the real (imaginary) part of the pole energy of the $\Lambda(1405)$ and the imaginary (real) part of the scattering length. Those resonance energies are slightly larger than the pole energy reported in Ref. [24]. Therefore as a last model, model (f) reproduces the deeper resonance energy $1406 - i25$ MeV of Ref. [24]. The scattering length of this model is $-1.72 + i0.44$ fm, which is, however, somewhat different from the value $-1.54 + i0.74$ fm in Ref. [24].

The $I = 1$ $\bar{K}N$ interaction is described by the $\bar{K}N$-$\pi\Sigma$-$\pi\Lambda$ coupled-channel model. The coupling constants $C_{\beta,\alpha}$ are $C_{\bar{K}N\text{-}\bar{K}N} = 2$, $C_{\bar{K}N\text{-}\pi\Sigma} = -2$, $C_{\bar{K}N\text{-}\pi\Lambda} = -\sqrt{6}$, $C_{\pi\Sigma\text{-}\pi\Sigma} = 4$, and $C_{\pi\Sigma\text{-}\pi\Lambda} = C_{\pi\Lambda\text{-}\pi\Lambda} = 0$. The cutoff Λ's are determined to fit the imaginary part of the scattering length of Ref. [22], which are given as model (A) in Tables III and IV for the nonrelativistic and relativistic models. The real part of the scattering length of those models is larger than $a_{\bar{K}N}^{I=1} = 0.37 + i0.60$ fm of Ref. [22]. The K^-p scattering length predicted from model (aA), which is model (a) for $I = 0$ and model (A) for $I = 1$ interactions, is between the central values of the two kaonic hydrogen data [25–27]. To study the sensitivity of the models of the $I = 1$ $\bar{K}N$

TABLE II. Same as Table I, but for the nonrelativistic models.

Model	$\bar{K}N$ (MeV)	$\pi\Sigma$ (MeV)	Scattering length (fm)	Resonance energy (MeV)
(a)	946	988	$-1.70 + i0.68$	$1420.1 - i30.1$
(b)	954	1035	$-1.60 + i0.68$	$1422.4 - i34.7$
(c)	940	944	$-1.80 + i0.68$	$1418.7 - i26.0$
(d)	968	933	$-1.70 + i0.58$	$1414.3 - i30.5$
(e)	927	1031	$-1.70 + i0.78$	$1424.7 - i29.0$
(f)	1000	800	$-1.72 + i0.43$	$1404.8 - i25.5$

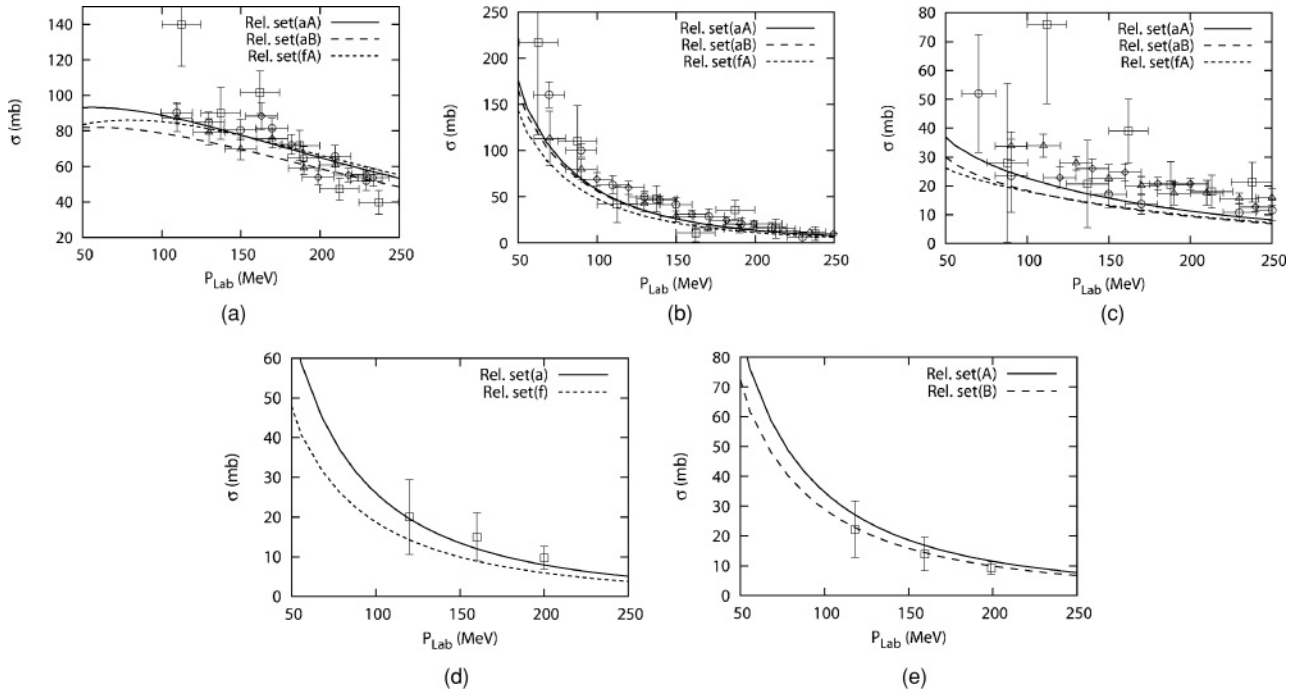

FIG. 6. Total cross section of (a) $K^- p \to K^- p$, (b) $K^- p \to \pi^+ \Sigma^-$, (c) $K^- p \to \pi^- \Sigma^+$, (d) $K^- p \to \pi^0 \Sigma^0$, and (e) $K^- p \to \pi^0 \Lambda$ reactions in the relativistic model. Data are from Refs. [29–33].

interaction to the resonance energy of the $K^- pp$ system, we constructed model (B) given in Tables III and IV. A similar model of $\bar{K}N$ interaction is developed to study $K^- d$ scattering [28]. The range of the vertex form factor found in in Ref. [28], which is a monopole form factor with 880 MeV cutoff mass, is comparable to ours.

The total cross sections of $K^- p$ reactions predicted from our models (aA), (aB), and (fA) are shown in Fig. 6 together with the data [29–33]. The models (aA) and (aB) describe well the $K^- p \to K^- p$ [Fig. 6(a)], $K^- p \to \pi^+ \Sigma^-$ [Fig. 6(b)], and $K^- p \to \pi^- \Sigma^+$ [Fig. 6(c)] reactions, where both $I = 0$ and $I = 1$ interactions contribute to the cross section. The models of $I = 0$ and $I = 1$ can be tested from $K^- p \to \pi^0 \Sigma^0$ [Fig. 6(d)] and $K^- p \to \pi^0 \Lambda$ [Fig. 6(e)] reactions, where models (a) and (A)/(B) describe the cross sections well. The model (fA) tends to give smaller cross sections. It is noticed, however, as we will see, that the resonance energy of the $K^- pp$ system is more sensitive to the $I = 0$ $\bar{K}N$ interaction and less sensitive to $I = 1$ interactions, while both $I = 0$ and $I = 1$ interactions are equally important in describing the $K^- p$ cross sections and kaonic hydrogen data.

The form of the s-wave πN interactions is taken as Eq. (25). The constant $C_{\alpha,\beta}$ is 4 for $I = 1/2$ and -2 for $I = 3/2$ states. The parameters of the potentials are determined by fitting the scattering length and the low energy phase shifts. For the $I = 1/2$ state, the strength of the potential is modified as $\lambda C_{\beta,\alpha}$ by introducing a phenomenological factor λ to describe the data of the scattering length $(0.1788 \pm 0.0050) m_\pi^{-1}$ [34] and the phase shifts [35]. The fitted parameters λ and Λ are shown in Table V together with the scattering length calculated using the models. The models describe well the S_{11} phase shifts up to 1.2 GeV as shown in Fig. 7.

For the $I = 3/2$ πN scattering, the πN potential is constructed so as to reproduce the scattering length $(-0.0927 \pm 0.0093) m_\pi^{-1}$ [34] and the S_{31} partial wave phase shifts data. Here we introduced a modified dipole form factor as

$$g(\vec{p}) = \frac{\Lambda^4}{(\vec{p}^2 + \Lambda^2)^2} \times (1 + a\vec{p}^2). \tag{26}$$

The parameters of the model are Λ and a for the form factor and the strength parameter λ. The obtained parameters are summarized in Table VI. The relativistic model can describe well the phase shifts up to 1.2 GeV as shown in Fig. 7; however,

TABLE III. Cutoff parameters, scattering lengths of the relativistic models of the $I = 1$, $\bar{K}N$-πY interaction.

Model	$\bar{K}N$ (MeV)	$\pi\Sigma$ (MeV)	$\pi\Lambda$ (MeV)	Scattering length (fm)
(A)	1100	850	1250	$0.68 + i0.60$
(B)	950	800	1250	$0.65 + i0.46$

TABLE IV. Same as Table III, but for the nonrelativistic models.

Model	$\bar{K}N$ (MeV)	$\pi\Sigma$ (MeV)	$\pi\Lambda$ (MeV)	Scattering length (fm)
(A)	920	960	640	$0.72 + i0.59$
(B)	800	940	660	$0.68 + i0.45$

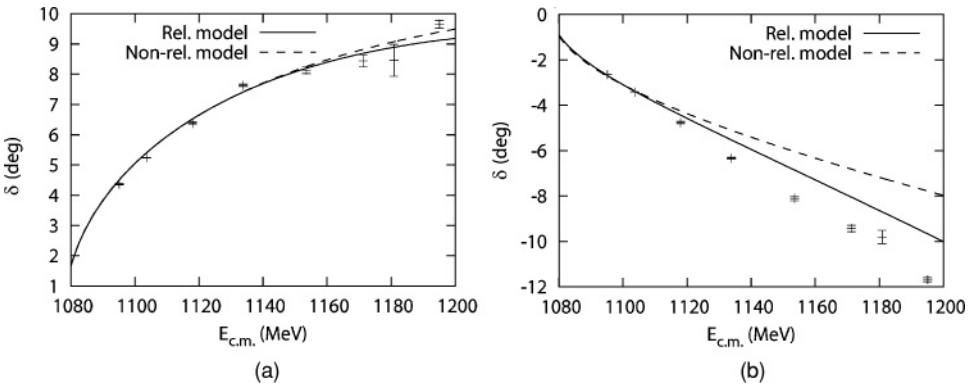

FIG. 7. Phase shift of the πN scattering for (a) S_{11} and (b) S_{31} partial waves. Data are from Ref. [35].

the nonrelativistic model starts to deviate from the data at around 1.1 GeV.

We used a Yamaguchi-type separable interaction for the nucleon-nucleon potential. To take into account the long range attractive interaction and the short range repulsion of the two-nucleon interaction, we used a two-term separable potential,

$$\langle \vec{p}'|V_{BB}|\vec{p}\rangle = C_R g_R(\vec{p}')g_R(\vec{p}) - C_A g_A(\vec{p}')g_A(\vec{p}). \quad (27)$$

Here C_R (C_A) is the coupling strength of the repulsive (attractive) potential. $g_R(\vec{p})$ [$g_A(\vec{p})$] is the form factor, whose form is given as $g_R(\vec{p}) = \Lambda_R^2/(\vec{p}^2 + \Lambda_R^2)$ [$g_A(\vec{p}) = \Lambda_A^2/(\vec{p}^2 + \Lambda_A^2)$], where Λ is a cutoff of the nucleon-nucleon potential. The adjustable parameters in our nucleon-nucleon potential are determined by fits to the data of the $^1S_0$ phase shifts [36]. The best-fit parameters are summarized in Table VII. The low energy phase shifts of the $^1S_0$ state is shown in Fig. 8.

IV. RESULTS AND DISCUSSION

The dibaryon resonance with $J^\pi = 0^-$, $S = -1$, $I = 1/2$ is studied using a formalism of the Faddeev equation as explained in Sec. II. We assume all the angular momentum to be in an s-wave state and the spin singlet state $S_{BB} = 0$ for the two-baryon states. We have included the dominant $\bar{K}NN$, $\pi\Sigma N$, and $\pi\Lambda N$ Fock-space components, whose isospin wave functions are $[\bar{K} \otimes [NN]_{I=1}]_{I=1/2}$, $[\pi \otimes [\Sigma N]_{I=1/2,3/2}]_{I=1/2}$, and $[\pi \otimes [\Lambda N]_{I=1/2}]_{I=1/2}$. An approximation within this model is that the weak YN interaction is not included.

Let us start to examine the three-body resonance energy by taking into account only the $\bar{K}N$ interactions $v^{I=0,1}_{\bar{K}N\text{-}\bar{K}N}$, neglecting the πYN Fock space. In this case, the bound state pole is expected to lie on the physical Riemann sheet below $m_K + 2m_N$ if the $\bar{K}N$ attraction is strong enough. Therefore it is not necessary to use the analytic continuation of the amplitude with the deformed contour discussed in Sec. II, so we simply use the integral over the momentum p_i in the real axis. The results are shown in Fig. 9 marked by a and a' for the relativistic and nonrelativistic models, respectively. Here we use the standard parameters (aA) of the $\bar{K}N$ interaction with nonrelativistic and relativistic kinematics. The binding energies are about 18 MeV. The $\bar{K}N$ interaction included in τ and Z is strong enough to bind the $\bar{K}NN$ system, where the $I = 0$ $\bar{K}N$ interaction plays a dominant role. We then take into account the NN interaction. Then the binding energy increases farther to 25.1 MeV (22.8 MeV) shown as b (b') for relativistic (nonrelativistic) model. Notice that if we neglect the repulsive component of the NN interaction, we obtain a much more deeply bound state.

In the next step, we gradually include the πYN interactions, while the pion-exchange Z diagram is not yet included. To do this, we multiply by factor x the coupling constants $C_{\alpha,\beta}$ of the $\bar{K}N$-πY and πY-πY interactions as $xC_{\alpha,\beta}$. When the parameter is zero, $x = 0$, the πY is disconnected from $\bar{K}N$; and when it takes the value 1, $x = 1$, we recover the full model. By varying the parameter x from 0 to 1, we can follow the trajectory of the resonance pole from the bound state pole. Now the $\bar{K}NN$ bound state decays into the πYN channel, and the bound state pole moves into the unphysical sheet. Since the $\bar{K}NN$ bound state was found above the $\pi\Sigma N$ threshold, the resonance pole may be on the πYN unphysical and $\bar{K}NN$ physical Riemann sheet, which we discussed in Sec. II. The results of the pole trajectories are shown by the solid and dashed curves in Fig. 9 corresponding to the relativistic and the nonrelativistic models. Increasing the coupling to the πYN channel causes the width as well as the binding energy of the resonance to increase. For larger binding energy $\mathrm{Re}(W_{\mathrm{pole}} - W_{KNN}) < -60$ MeV, the width starts to decrease because of

TABLE V. Parameters and scattering lengths for the relativistic and nonrelativistic models of the $I = 1/2$, πN interaction.

Model	λ	Λ7 (MeV)	Scattering length
Relativistic	0.90	800	$0.175m_\pi^{-1}$
Nonrelativistic	0.85	800	$0.177m_\pi^{-1}$

TABLE VI. Parameters and scattering lengths for the relativistic and nonrelativistic model of the $I = 3/2$, πN interaction.

Model	λ	Λ (MeV)	a (fm)^2	Scattering length
Relativistic	2.7	618	0.50	$-0.095m_\pi^{-1}$
Nonrelativistic	3.0	628	0.30	$-0.101m_\pi^{-1}$

TABLE VII. Our parameters of the relativistic and nonrelativistic models for NN scattering.

Model	Λ_R (MeV)	Λ_A (MeV)	C_R (MeV fm^3)	C_A (MeV fm^3)
Relativistic	1144	333	5.33	5.61
Nonrelativistic	1215	352	5.05	5.84

the decreasing phase space for the decay into the $\pi\Sigma N$ state. The pole position is at $-82 - i29$ MeV $(-91 - 28i)$ for the relativistic (nonrelativistic) model shown as $c(c')$. It is noticed that the numerical method used to follow the pole trajectories helps us determine whether we encounter singularities or not. As an example, the pole of the three-body resonance is shown by the solid line in Fig. 10 for $0 < x < 1$. The pole of the $\Lambda(1405)$ is also shown by the dashed curve. The trajectory of the $\bar{K}NN$ resonance is similar to case A in Fig. 5, and the integration contour does not intercept the singularity arising from the two-body resonance $\Lambda(1405)$.

Finally, we include the π exchange mechanism in Z and πN two-body scattering terms in τ, which adds another mechanism for the decay of the $\bar{K}NN$ into πYN and is important for the width of the three-body resonance. The final results of the $\bar{K}NN$-πYN resonance poles are denoted by d and d' in Fig. 9. This mechanism increases the width of the three-body resonance by about 14 MeV, while the effect on the real part is small. The cancellation between the attractive $I = 1/2$ πN interaction and the repulsive $I = 3/2$ πN interaction may lead to small effects on the real part of the resonance energy. The effects of the $\pi\Lambda N$ channel are small and increase the binding energy and half-width at most by 1 MeV. The pole position of the three-body resonance is $W = M - i\Gamma/2 = 2m_N + m_K - 79.3 - i37.1$ MeV $(2m_N + m_K - 92.2 - i35.4$ MeV) for the relativistic (nonrelativistic) model, shown as d and d'.

The model dependence of our results on the three-body resonance is summarized in Tables VIII and IX. The $\bar{K}NN$-πYN resonance pole is located on the $\bar{K}NN$ physical and πYN unphysical sheet with the binding energy $B \sim 60$–95 MeV and the width $\Gamma \sim 45$–80 MeV, using relativistic models. All of our models predict resonance energies above

TABLE VIII. Pole energy $(W_{\rm pole} - m_K - 2m_N)$ of the three-body resonance using relativistic models. The listed pole energies in MeV can be related to binding energy B and the width Γ as $W_{\rm pole} - m_K - 2m_N = -B - i\Gamma/2$.

	Model (A)	Model (B)
(a)	$-79.3 - i37.1$	$-79.3 - i37.3$
(b)	$-93.3 - i27.4$	$-93.3 - i27.6$
(c)	$-57.2 - i38.6$	$-56.9 - i38.6$
(d)	$-72.4 - i31.7$	$-72.2 - i31.9$
(e)	$-87.1 - i40.8$	$-87.1 - i41.0$
(f)	$-63.3 - i22.2$	$-63.2 - i22.3$

TABLE IX. Same as Table VIII, but for the nonrelativistic models.

	Model (A)	Model (B)
(a)	$-92.2 - i35.4$	$-92.3 - i35.6$
(b)	$-101.6 - i20.7$	$-101.6 - i20.7$
(c)	$-72.7 - i53.9$	$-72.5 - i54.9$
(d)	$-83.0 - i33.3$	$-83.0 - i33.6$
(e)	$-98.1 - i33.2$	$-98.2 - i33.3$
(f)	$-66.5 - i24.4$	$-66.3 - i24.4$

the $\pi\Sigma N$ threshold. The relatively large model dependence of our results is due to the uncertainty in the models of the $I = 0$, $\bar{K}N$-$\pi\Sigma$ interaction. Comparing the results of model (A) with model (B), we can see the three-body pole position is almost independent of the parameters of the $I = 1$, $\bar{K}N$-πY interaction. By varying the real (imaginary) part of the fitted scattering length by ± 0.1 fm, the binding energy of the three-body resonance is affected by $\sim \pm 14(8)$ MeV. Following another way to construct the model, the parameters of model (f) are fitted to the pole energy of $\Lambda(1405)$. This model predicts the scattering length $-1.72 + i0.44$ fm. The energy of the three-body resonance is found to be $B = 63$ MeV with a rather small width, $\Gamma = 44$ MeV, compared with models (a)–(e), which can already be seen in the small imaginary part of the scattering length in model (f).

Let us briefly compare our results with those of the other theoretical studies of the $K^- pp$ resonance, which use a nonrelativistic approach. Our resonance has a deeper binding energy and a similar width compared with those in Ref. [4]. However, it is not straightforward to compare our results with the pole energy of Ref. [4] because of the differences in the methods used to obtain the three-body resonance energy and the model for the $\bar{K}N$ interaction. Their $\bar{K}N$ potential is stronger and has a shorter range than ours. Recently Shevchenko, Gal, and Mares [19] studied $K^- pp$ system using the nonrelativistic coupled-channel Faddeev equation. Though the details of their method is not described in Ref. [19], it seems their approach is quite similar to our present study. They employed a phenomenological $\bar{K}N$ potential model and reported $B \sim 55$–70 MeV and $\Gamma \sim 95$–110 MeV. Their result is consistent with our results of the nonrelativistic model. Specially our result using model (c) gives a quite similar resonance energy and width.

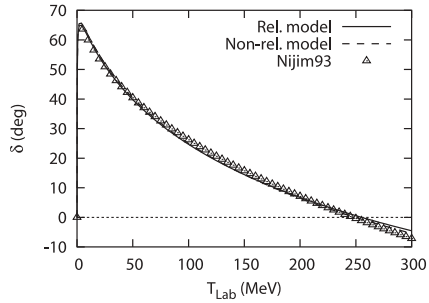

FIG. 8. Phase shifts of NN scattering for the $^1S_0$ state. The phase shifts calculated from the model of Ref. [36] are shown in triangles.

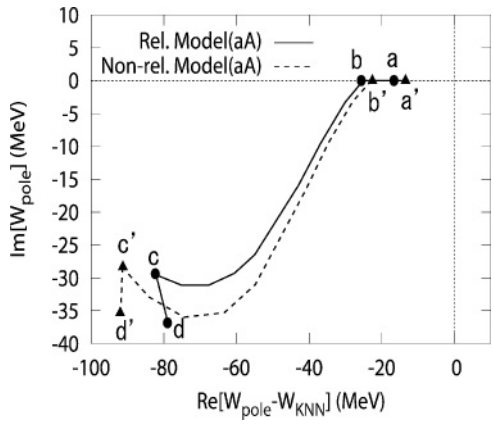

FIG. 9. Pole trajectories of the $\bar{K}NN$-πYN scattering amplitude for the $J^\pi = 0^-$ and $I = 1/2$ state. Filled circles (filled triangles) show the results of the relativistic (nonrelativistic) model (aA) for different steps in the analysis, as explained in the text. Here $W_{KNN} = m_K + 2m_N$.

In summary, we have studied the existence and properties of a strange dibaryon resonance using the $\bar{K}NN$-πYN coupled-channel Faddeev equation. By solving the three-body equation, the energy dependence of the resonant $\bar{K}N$ amplitude is fully taken into account. The resonance pole has been investigated from the eigenvalue of the kernel with the analytic continuation of the scattering amplitude on the unphysical Riemann sheet. The model of the $\bar{K}N$-πY interaction is constructed from the leading order term of the chiral Lagrangian and takes into account the relativistic kinematics. The $\bar{K}N$ interaction parameters are fitted to the scattering length given by Martin [22]. We found a resonance pole at $B \sim 79$ MeV and $\Gamma \sim 74$ MeV in the relativistic model (aA). However, as the $\bar{K}N$ interaction is not very well constrained by the data, we studied a possible range of the resonance energies by considering different parameter sets of the $\bar{K}N$-πY interaction. The binding energy and the full width can be in the range of $B \sim 60$–95 MeV and $\Gamma \sim 45$–80 MeV when computed in the relativistic model. To connect the resonance found in this work to the experimental signal, further theoretical studies on the production mechanism and further decay of the resonance especially to the Λ-p channel are necessary.

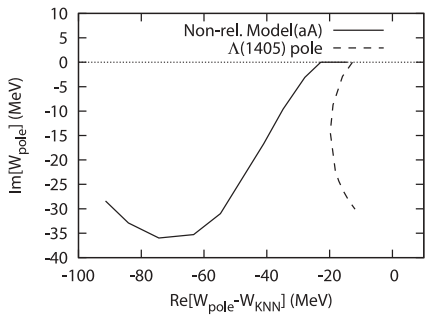

FIG. 10. Pole trajectories of the three-body resonance and $\Lambda(1405)$ using the nonrelativistic model (aA).

ACKNOWLEDGMENTS

The authors are grateful to Prof. A. Matsuyama for very useful discussions on the three-body resonance. We also thank Drs. B. Juliá-Díaz and T.-S. H. Lee and Prof. A. Gal for discussions. This work is supported by a Grant-in-Aid for Scientific Research on Priority Areas (MEXT), Japan, No. 18042003.

APPENDIX

The spin-isospin recoupling coefficient of the particle exchange interaction Z is briefly explained. The coefficient given in Eq. (1.181) of Ref. [21] can be simplified for s-wave states. The three-body state with total spin and isospin $(S_{\rm tot}, I_{\rm tot})$, which couples with the baryon "isobar" with spin and isospin (S, I) and the spectator baryon $B_{i(S_i,I_i)}$, is given as

$$|[[M_{3(S_3,I_3)} \otimes B_{j(S_j,I_j)}]_{(S,I)} \otimes B_{i(S_i,I_i)}]_{(S_{\rm tot},I_{\rm tot})}\rangle. \quad \text{(A1)}$$

Here baryon i, j represents particle 1 or 2, and the meson is always assigned as the third particle. The wave function of the three-body state, which couples with the dibaryon isobar and the spectator meson M_3, is given as

$$|[[B_{1(S_1,I_1)} \otimes B_{2(S_2,I_2)}]_{(S,I)} \otimes M_{3(S_3,I_3)}]_{(S_{\rm tot},I_{\rm tot})}\rangle. \quad \text{(A2)}$$

Then Eq. (7) is extended to include spin-isospin degrees of freedom. The particle exchange interaction for the spectators l, m, the isobars f', f with spin-isospin (S', I') and (S, I), and the exchanged particle n can be expressed as

$$\begin{aligned} &Z_{l,f'(S',I'),m,f(S,I)}(p_l, p_m, W) \\ &\quad = R_{l,f'(S',I'),m,f(S,I)} \int d(\hat{p}_l \cdot \hat{p}_m) \\ &\qquad \times \frac{2\pi g_{f'(S',I')}(q_l) g_{f(S,I)}(q_m)}{W - E_l(p_l) - E_m(p_m) - E_n(\vec{p}_l + \vec{p}_m)}, \end{aligned} \quad \text{(A3)}$$

where f represents isobar Y_K, Y_π, d, and N^*.

$R_{l,f'(S',I'),m,f(S,I)}$ is given by the overlap of the initial and final spin-isospin wave functions. For the meson (M_3) exchange mechanism, $R_{i,f'(S',I'),j,f(S,I)}$ is given as

$$\begin{aligned} R_{i,f'(S',I'),j,f(S,I)} &= \langle [[M_{3(S_3,I_3)} \otimes B_{j(S_j,I_j)}]_{(S',I')} \\ &\quad \otimes B_{i(S_i,I_i)}]_{(S_{\rm tot},I_{\rm tot})} | [[M_{3(S_3,I_3)} \\ &\quad \otimes B_{i(S_i,I_i)}]_{(S,I)} \otimes B_{j(S_j,I_j)}]_{(S_{\rm tot},I_{\rm tot})} \rangle \\ &= (-1)^{S+S'-S_3-S_{\rm tot}} W(S_i, S_3, S_{\rm tot}, S_j; S, S') \\ &\quad \times \sqrt{(2S+1)(2S'+1)} (-1)^{I+I'-I_3-I_{\rm tot}} \\ &\quad \times W(I_i, I_3, I_{\rm tot}, I_j; I, I') \\ &\quad \times \sqrt{(2I+1)(2I'+1)}. \end{aligned} \quad \text{(A4)}$$

For the baryon (B_j) exchange mechanism, $R_{i,f'(S',I'),3,f(S,I)}$ is given as

$$
\begin{aligned}
&R_{i,f'(S',I'),3,f(S,I)} \\
&\quad = \langle [[M_{3(S_3,I_3)} \otimes B_{j(S_j,I_j)}]_{(S',I')} \otimes B_{i(S_i,I_i)}]_{(S_{\rm tot},I_{\rm tot})}| \\
&\qquad \times [[B_{1(S_1,I_1)} \otimes B_{2(S_2,I_2)}]_{(S,I)} \otimes M_{3(S_3,I_3)}]_{(S_{\rm tot},I_{\rm tot})}\rangle \\
&\quad = (-1)^{S_3+S-S_{\rm tot}+I_3+I-I_{\rm tot}} \\
&\qquad \times W(S_3, S_j, S_{\rm tot}, S_i; S', S)\sqrt{(2S'+1)(2S+1)} \\
&\qquad \times W(I_3, I_j, I_{\rm tot}, I_i; I', I)\sqrt{(2I'+1)(2I+1)} \\
&\qquad \times \left(\delta_{i,2}\delta_{j,1} + \delta_{i,1}\delta_{j,2}(-1)^{S_i+S_j-S+I_i+I_j-I}\right). \qquad \text{(A5)}
\end{aligned}
$$

When we antisymmetrize the AGS equation, the last factor in the bracket in Eq. (A5) projects the antisymmetric two-nucleon states. This can be explicitly seen by comparing the exchange of nucleon 2 $Z_{2,Y_K(S',I'),3,d(S,I)}$ and nucleon 1 $Z_{1,Y_K(S',I'),3,d(S,I)}$ interactions. Using Eq. (A5), those interactions are related as

$$R_{1,Y_K(S',I'),3,d(S,I)} = (-1)^{S+I} R_{2,Y_K(S',I'),3,d(S,I)}, \qquad \text{(A6)}$$

which leads to Eq. (17) as

$$X_{Y_K,Y_K} = (1-(-1)^{S+I}) Z_{Y_K,d}\tau_{d,d} X_{d,Y_K} + \cdots. \qquad \text{(A7)}$$

[1] J. Mares, E. Friedman, and A. Gal, Nucl. Phys. **A770**, 84 (2006).
[2] L. Tolós, A. Ramos, and E. Oset, Phys. Rev. C **74**, 015203 (2006).
[3] Y. Akaishi and T. Yamazaki, Phys. Rev. C **65**, 044005 (2002).
[4] T. Yamazaki and Y. Akaishi, Phys. Lett. **B535**, 70 (2002).
[5] A. Dote, H. Horiuchi, Y. Akaishi, and T. Yamazaki, Phys. Rev. C **70**, 044313 (2004).
[6] M. Agnello *et al*., Phys. Rev. Lett. **94**, 212303 (2005).
[7] V. K. Magas, E. Oset, A. Ramos, and H. Toki, Phys. Rev. C **74**, 025206 (2006).
[8] W. Glöckle, Phys. Rev. C **18**, 564 (1978).
[9] K. Möller, Czech. J. Phys. **32**, 291 (1982).
[10] A. Matsuyama and K. Yazaki, Nucl. Phys. **A534**, 620 (1991); A. Matsuyama, Phys. Lett. **B408**, 25 (1997).
[11] I. R. Afnan and A. W. Thomas, Phys. Rev. C **10**, 109 (1974).
[12] B. C. Pearce and I. R. Afnan, Phys. Rev. C **30**, 2022 (1984).
[13] I. R. Afnan and B. F. Gibson, Phys. Rev. C **47**, 1000 (1993).
[14] J. A. Oller and U.-G. Meißner, Phys. Lett. **B500**, 263 (2001).
[15] D. Jido *et al*., Nucl. Phys. **A725**, 181 (2003).
[16] B. Borasoy, R. Nißler, and W. Weise, Eur. Phys. J. A **25**, 79 (2005).
[17] T. Hamaie, M. Arima, and K. Masutani, Nucl. Phys. **A591**, 675 (1995).
[18] Y. Ikeda and T. Sato, arXive:nucl-th/0701001.
[19] N. V. Shevchenko, A. Gal, and J. Mares, Phys. Rev. Lett. **98**, 082301 (2007).
[20] E. O. Alt, P. Grassberger, and W. Sandhas, Nucl. Phys. **B2**, 167 (1967).
[21] I. R. Afnan and A. W. Thomas, in *Modern Three-Hadron Physics*, edited by A. W. Thomas (Springer, Berlin, 1977), Chap. 1.
[22] A. D. Martin, Nucl. Phys. **B179**, 33 (1981).
[23] B. Borasoy, U.-G. Meiszner, and R. Niszler, Phys. Rev. C **74**, 055201 (2006).
[24] R. H. Dalitz and A. Deloff, J. Phys. G **17**, 289 (1991).
[25] M. Iwasaki *et al*., Phys. Rev. Lett. **78**, 3067 (1997).
[26] T. M. Ito *et al*., Phys. Rev. C **58**, 2366 (1998).
[27] G. Beer *et al*., Phys. Rev. Lett. **94**, 212302 (2005).
[28] A. Bahaoui, C. Fayard, T. Mizutani, and B. Saghai, Phys. Rev. C **68**, 064001 (2003).
[29] W. E. Humphrey and R. R. Ross, Phys. Rev. **127**, 1305 (1962).
[30] M. Sakitt *et al*., Phys. Rev. **139**, B719 (1965).
[31] J. K. Kim, Phys. Rev. Lett. **14**, 29 (1965).
[32] W. Kittel, G. Otter, and I. Wacek, Phys. Lett. **B21**, 349 (1966).
[33] D. Evans *et al*., J. Phys. G **9**, 885 (1983).
[34] H.-Ch. Schröder *et al*., Phys. Lett. **B469**, 25 (1999).
[35] R. A. Arndt, I. I. Strakovsky, R. L. Workman, and M. M. Pavan, Phys. Rev. C **52**, 2120 (1995); R. A. Arndt, I. I. Strakovsky, and R. L. Workman, Int. J. Mod. Phys. A **18**, 449 (2003).
[36] V. G. J. Stoks, R. A. M. Klomp, C. P. F. Terheggen, and J. J. de Swart, Phys. Rev. C **49**, 2950 (1994).